Supplementary Material (ESI) for Chemical Communications

Novel spin transition between S = 5/2 and S = 3/2 in highly saddled iron(III) porphyrin complexes at extremely low temperature

Yoshiki Ohgo,*[a,f] Yuya Chiba,[b] Daisuke Hashizume,[c] Hidehiro Uekusa,[d] Tomoji Ozeki, [d] and Mikio Nakamura*[a,e,f]

[a]*Department of Chemistry, School of Medicine, Toho University, Ota-ku, Tokyo 143-8540, Japan. E-mail: yohgo@med.toho-u.ac.jp; mnakamu@med.toho-u.ac.jp*

[b]*Division of Biomolecular Science, Graduate School of Science, Toho University, Funabashi 274-8510, Japan.*

[c]*Molecular Characterization Team, RIKEN, Wako, Saitama 351-0198, Japan*

[d]*Graduate School of Science and Engineering, Tokyo Institute of Technology*

[e]*Division of Chemistry, Graduate School of Science, Toho University, Funabashi 274-8510, Japan.*

[f]*Research Center of Materials with Integrated Properties, Toho University, Funabashi, 274-8510, Japan*

Supplementary Information

1. EPR Spectra: The temperature dependent EPR spectra of **1** and **2** taken in CH_2Cl_2 solution and in the solid, respectively, are given in **Fig. 3** of the article. **Fig S-1** given below shows the temperature dependent EPR spectra of **1** and **2** taken in the solid and in CH_2Cl_2 solution, respectively. Obviously, both **1** and **2** exhibit the spin transition in solution as well as in the solid. Close inspection of these figures reveals, however, that the spin transition occurs more completely in the solid than in solution. For example, the population of the high-spin species of **1** changes from 0 (70 K) to 4 %(1.5 K) in solution as shown in **Fig. 3(a)**, while it changes from 0 (20 K) to 21 %(1.6 K) in the solid as shown in **Fig. S-1(a)**. Similar tendency is also seen in **2**. The results strongly indicate that the structural change in the crystal lattice at lower temperature enhances the spin transition as described in the article.

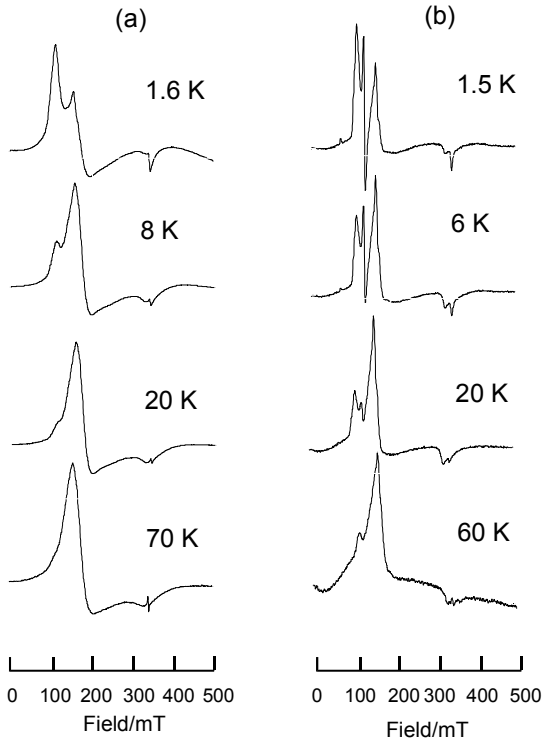

Fig. S-1 EPR spectra of (a) **1** taken in the solid, and (b) **2** taken in CH_2Cl_2 solution at various temperatures.

2. Crystal Structures: **Fig S-2** shows the packing diagrams of **1** viewed along (a) b-axis and (b) a-axis, and **2** viewed along (c) a-axis and (d) c-axis. As shown in these figures, there are the porphyrin arrays in which molecules are aligned in a 2-fold symmetry along a-axis. The molecules are connected by alternately existing (A) hydrogen bonding between H_2O and ClO_4^-, and (B) hydrogen bonding between ClO_4^- and H_2O of the neighboring molecule at (x+1/2, -y+3/2, -z+1). Thus, the long hydrogen bonding chain exists along the a-axis, which is consisting with repetition of …(H_2O)…(ClO_4^-)…$(H_2O)^*$ …$(ClO_4^-)^*$…, where $(H_2O)^*$ and $(ClO_4^-)^*$ are the neighboring water molecule and counter anion represented in a symmetry code (x+1/2, -y+3/2, -z+1).

In contrast to the case of **1**, the complex **2** exists as discrete dimeric structures. Each dimeric structure is stabilized by the hydrogen bondings consisting of the coordinated H_2O molecules and ClO_4^- anions as shown below. As the temperature is lowered, the unit cell volume is expected to shrink. Because **1** and **2** have highly saddled structure with bulky substituents at the porphyrin periphery as illustrated in Scheme 1, the shrinkage of the unit cell could directly affect each molecule from the lateral side. Under the circumstances, each molecule of **2** suffers packing force easily from a- and c- axes that are almost coincide with the lateral (equatorial) directions of the molecules. On the other hand, the dimeric unit could resist the packing force from the axial direction because of the severe steric hindrance between bulky alkyl substituents. As a result, the narrow N4 cavities of **1** and **2** would further decrease at extremely low temperature, which could extrude the iron(III) ion away from the N4 plane and induce the spin transition from the S=3/2 to the S=5/2.

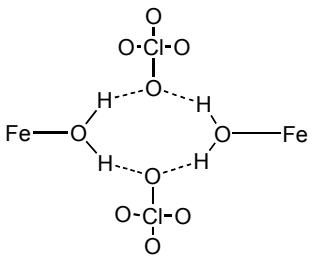

(a) (b)

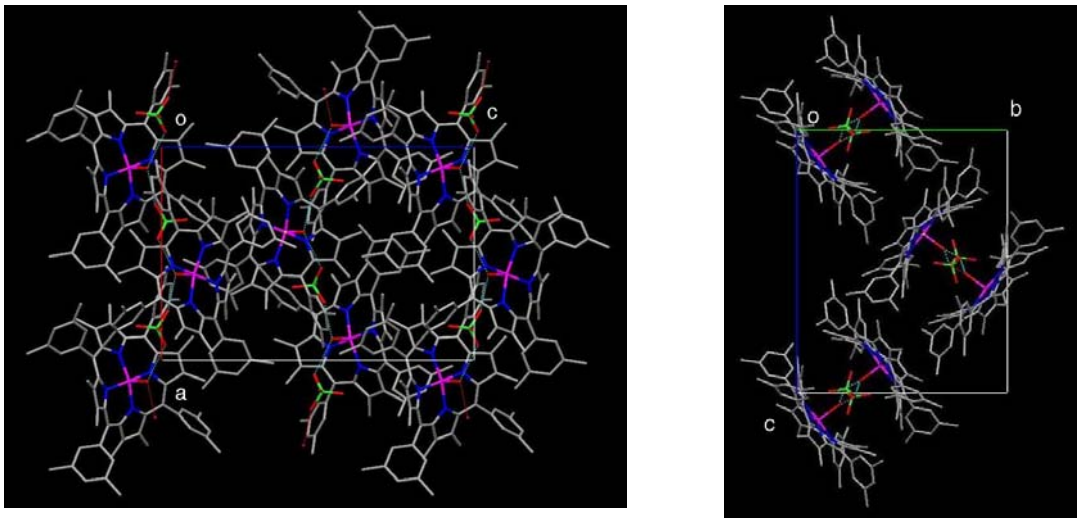

(c) (d)

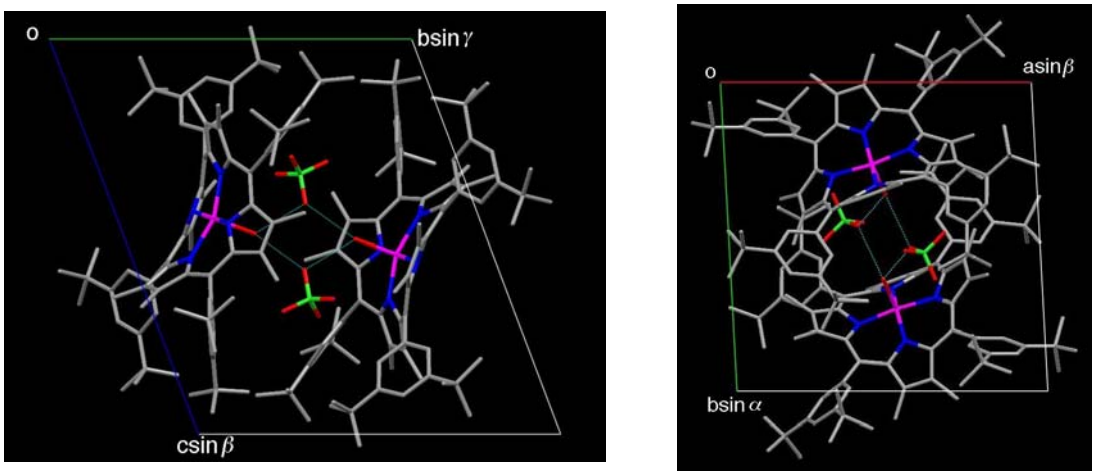

Fig S-2. Packing diagrams of **1** viewed along (a) b-axis and (b) c-axis, and **2** viewed along (c) a-axis and (d) c-axis.